Conference paper

Francesca Baldassarre[a,]*, Angelo De Stradis[a], Giuseppe Altamura, Viviana Vergaro, Cinzia Citti, Giuseppe Cannazza, Agostina L. Capodilupo, Luciana Dini and Giuseppe Ciccarella*

Application of calcium carbonate nanocarriers for controlled release of phytodrugs against *Xylella fastidiosa* pathogen

https://doi.org/10.1515/pac-2018-1223

Abstract: Calcium carbonate-based hollow or porous particles are one of the preferred carriers for fabrication of drug delivery systems. We have developed an eco-friendly method to produce calcium carbonate nanocrystals, which have shown biocompatibility and optimal capacity to across cell membrane in human cell lines providing new tools in cancer therapy. The success of drug delivery systems has paved the way for the development of systems for controlled release of agrochemicals. In this work, we exploited calcium carbonate nanocrystals as carriers for targeted release of phytodrugs investigating a potential control strategy for the pathogen *Xylella fastidiosa*. This pathogen is the causal agent of the Olive Quick Decline Syndrome that is an unprecedented emergency in Italy and potentially in the rest of Europe. We studied nanocrystals interactions with bacteria cells and the application in planta to verify olive plants uptake. Ultrastructural analysis by electron microscopy shown an alteration of bacteria wall following nanocrystals interaction. Nanocrystals were adsorbed from roots and they translocated in plants tissues. Calcium carbonate carriers were able to encapsulate efficiently two types of antimicrobial substances and the potential efficacy was tested in experiment under greenhouse conditions.

Keywords: calcium carbonate; drug delivery; electron microscopy; Eurasia 2018; nanocrystals; phytodrug; plants; *Xylella fastidiosa*.

Article note: A collection of invited papers based on presentations at the 15th Eurasia Conference on Chemical Sciences (EuAsC2S-15) held at Sapienza University of Rome, Italy, 5–8 September 2018.

[a]**Francesca Baldassarre and Angelo De Stradis:** These authors contributed equally to this work.
***Corresponding authors: Francesca Baldassarre and Giuseppe Ciccarella,** Biological and Environmental Sciences Department, UdR INSTM of Lecce University of Salento, Via Monteroni, 73100 Lecce, Italy; and Institute of Nanotechnology, CNR NANOTEC, Consiglio Nazionale delle Ricerche, Via Monteroni, 73100 Lecce, Italy, e-mail: francesca.baldassarre@unisalento.it (F. Baldassarre); giuseppe.ciccarella@unisalento.it (G. Ciccarella)
Angelo De Stradis and Giuseppe Altamura: Institute for Sustainable Plant Protection, CNR – IPSP, Consiglio Nazionale delle Ricerche, Via Amendola 165/A, 70126 Bari, Italy
Viviana Vergaro: Biological and Environmental Sciences Department, UdR INSTM of Lecce University of Salento, Via Monteroni, 73100 Lecce, Italy; and Institute of Nanotechnology, CNR NANOTEC, Consiglio Nazionale delle Ricerche, Via Monteroni, 73100 Lecce, Italy
Cinzia Citti and Giuseppe Cannazza: Department of Life Sciences, University of Modena and Reggio Emilia, Via G. Campi 103, 41125 Modena, Italy; and Institute of Nanotechnology, CNR NANOTEC, Consiglio Nazionale delle Ricerche, Via Monteroni, 73100 Lecce, Italy
Agostina L. Capodilupo: Institute of Nanotechnology, CNR NANOTEC, Consiglio Nazionale delle Ricerche, Via Monteroni, 73100 Lecce, Italy
Luciana Dini: Department of Biology and Biotechnology “Charles Darwin”, University of Rome “La Sapienza”, Piazzale Aldo Moro 5, 00185 Roma, Italy

Introduction

Calcium carbonate ($CaCO_3$) is one of the most abundant biominerals and it has attracted considerable attention as smart low price material in many research and development fields. The properties and applications of $CaCO_3$ depend on its morphology, particles size, crystal phase and growth. Therefore, $CaCO_3$ micro and nanoparticles synthesis was widely investigated for different research and industrial aims. Calcium carbonate has no toxicity and its use was exploited for many applications in cosmetics, medicine and agrofood industry [1]. $CaCO_3$-based hollow or porous particles are preferred for drug delivery vehicles fabrication as indicated from recent publications [2, 3]. The micro and nanosized materials provide significantly improved proprieties and functionalities so their design has become crucial for industrial and biotechnological applications. The success of nanomedicine has paved the way for the development of agri-nanotechnology [4, 5]. The design of slow release systems based on micro and nanostructured materials, is a powerful tool to overcome the problems related to conventional phytodrugs [6]. Usually, plants pathogens and pests are controlled by massive pesticide applications, 90 % of which are dispersed into the environment during application and following leaching phenomena. These critical issues have great negative impact on environmental and economic sustainability of the food chain production. Furthermore, the intense use of pesticides is known to cause pathogen resistance phenomena [7]. In this context, sustainable management of crops is essential and nanomaterials may represent valuable solutions to enhance plants growth and improve diseases resistance and control ensuring low environmental impact [8]. Nanomaterials provide many benefits such as improvement of efficacy due to higher surface area, higher bioavaibility, lower toxicity and in situ gradual release. The large surface/volume ratio allows the transport of higher concentrations of active substance to the target reducing the amount of pesticide required for pest control. Different nanostructured materials, nanoparticles, nanoclays and nanoemulsions, are used in agro food industry. Smart delivery systems are exploited for the controlled release of fertilizers, fungicides, insecticides, herbicides, pesticides. Different nanocarriers have proved to be suitable for slow release of agrochemicals ensuring protection from chemical and biological degradation. Molecules and/or macromolecules can be loaded into carriers through physical adsorption on nanoparticles, chemical attachment on nanoparticles or encapsulated inside nanomaterials [4, 9, 10]. Many types of nanoparticles are designed for parasitic weeds, pests and plant pathogens control [11–13]. Metal-based materials such as metal nano-oxides or nanocomposites are among the most investigated antimicrobial products [14–16]. Silver nanoparticles (AgNPs) strongly inactivate a variety of bacterial pathogens, both Gram-positive and Gram-negative, fungal pathogens and viruses and have been mainly exploited for biomedical applications [17–20]. AgNPs have been utilized as novel nanopesticide in many research studies to control plant diseases [21, 22]. Another type of nanomaterials with a strong antibacterial activity are nano-TiO_2, alumina particles and Cu compounds, which are exploited as antibacterial and antifungal substances for crop disease control [23–25]. However, the application of metal-based phytodrugs turned out to produce damages under some conditions and to be toxic on the plants and environment. Some studies shown damages to plants cells following metal nanoparticles uptake, such as Zn, Ag and Cu NPs [26–28]. Therefore, the research of additional nanomaterials is still a current topic to develop new systems with no toxicity and preferably biodegradable [29, 30]. In this work, calcium carbonate based nanocarriers (nano$CaCO_3$) were tested as innovative phytodrugs delivery systems. Previous works have reported the smart synthesis of nano$CaCO_3$ and have shown their improved proprieties as optimal systems for drugs controlled release [31–34]. The aim of this work was to test the use of nanocrystals to control the plant pathogenic bacterium *Xylella fastidiosa* in infected plants. The unexpected emergence of *X. fastidiosa* in the Salento peninsula (southern Italy) resulted in a dramatic phytosanitary situation due to the impact of bacterial infections on susceptible olive trees, the major affected host species in the Salento outbreaks. The epidemic spread in one of the major Italian olive-growing area has caused extensive and severe losses of olive trees, with dramatic impact not only on the olive crops but also for the landscape, characterized mainly by ancient and monumental olive trees [35–37]. *Xylella fastidiosa* is a Gram-negative bacterium whose pathogenicity is linked to its capacity to colonize and form a biofilm in the xylem vessels blocking the passage of water and nutrients from the roots to the canopy [38]. Therefore, several studies have been conducted on bacterial homeostasis and its interaction with plant

and vectors in order to investigate new containment strategies [39, 40]. To control and reduce the multiplication of the bacterium in the host plants, particular attention has been given to small molecules that could reach the xylem and potentially inhibit the proliferation of the bacterial cells and/or the biofilm formation. Among these molecules, the secondary metabolites play an important role for plants resistance to disease. Many phenolics, including p-coumaric acid, caffeic acid, ferulic acid and sinapic acid, have shown in vitro antimicrobial activities. Maddox et al. reported the inhibitory effects of 12 phenolic compounds towards four *X. fastidiosa* strains [41]. de Souza et al. reported the first investigation of the effect of N-acetylcysteine (NAC) as anti-biofilm agent, to control plants pathogen. Encouraging results were obtained in *Xylella*-infected citrus plants by hydroponic applications of NAC-Fertilizer [42]. In the present work we explored the possibility to use nanoCaCO$_3$ as a tool for the control of *X. fastidiosa*, either causing direct damages on the viability of the bacterial cells or as carrier of different antimicrobial molecules (i.e. NAC and caffeic acid). Nanocrystals were shown to interact with bacteria cells altering their membranes structure, and their fluorescence functionalization confirmed that they could be absorbed and translocated from the roots to stems and leaves of treated plants. Indeed the loading efficiency recorded for two selected substances was consistently high.

Experimental

Materials

All chemicals and organic solvents were of the highest purity commercially available from Sigma–Aldrich and TAAB Laboratories Equipment Ltd, Aldermaston, Berks, GB for electron microscopy.

NanoCaCO$_3$ synthesis

The CaCO$_3$ nanocrystals were synthesized as previous described [33]. Briefly a water solution of CaCl$_2$ (0.083 M) was mixed with a water solution of NaHCO$_3$ (0.125 M) using the instrument Büchi Mini Spray Dryer B-290. The CaCO$_3$ powder was collected and washed with H$_2$O, centrifuging (6000 rpm for 5 min) to remove the by-product NaCl and the resulting product was stably stored at room temperature until its utilization.

Fluorescent nanoCaCO$_3$ preparation

Fluorescent nanoCaCO$_3$ are used to evaluate the effective nanoparticles uptake and translocation within olive seedlings. The selected fluorescent probe is the TK-Lyso organic dye that is synthetized as reported by Capodilupo et al. [44]. The hydrophobicity of TK-Lyso was exploited for the adsorption on nanoCaCO$_3$ surface under following conditions: room temperature, overnight, dye concentration of 0.05 mg/mL for 100 mg of nanocrystals in water. UV-Vis absorption spectra were recorded on a Varian-Cary 500 spectrophotometer. The fluorescence spectra measurements were performed using a Varian Cary Eclipse spectrofluorimeter at the excitation wavelength of 405 nm.

Phytodrugs loading

The loading of caffeic acid within nanocarriers was carried out by adding, drop by drop, an ethanolic solution of phenolic compound (8 mM) to an aqueous solution (pH 7.5) of nanoCaCO$_3$ (100 mg) reaching the selected final concentrations (100 μM, 200 μM, 400 μM, 800 μM). The nanoCaCO$_3$ suspension was sonicated for 10 min prior loading. The physical adsorption was carried out mixing overnight the suspension at RT, in

the dark. The feed concentrations were chosen in line with the in vitro test of phenolic compounds that is reported by Maddox et al. [41]. The NAC loading was obtained through physical adsorption mixing the suspension of nanocrystals (100 mg) with two different NAC solutions (6 mg/mL and 20 mg/mL) overnight at RT. The pH of NAC solutions was adjusted to 7.5 adding NaOH 1 M and nano$CaCO_3$ suspension was sonicated for 10 min prior loading. NAC concentrations were established considering the in vitro experiment that was carried out on *X. fastidiosa* strain 9a5c [42]. The sample precipitation was collected following centrifugation (6000 rpm for 10 min) and supernatants were stored for the efficiency loading quantification. After three washing, the nanocrystals were dried in a stove at 50 °C.

Quantification of loading efficiency

Phytodrugs concentration in supernatants was quantified for the valuation of percentages loading efficiency according the following equation:

$$\%\ \text{loading efficiency} : 100 - ([\text{supernatant}]/[\text{loading solution}] * 100)$$

where the [supernatant] is the not loaded drug concentration and the [loading solution] is the initial concentration that was set for absorption experiment.

The amount of the caffeic acid supernatants was quantified recording UV-Vis absorption spectra at 311 nm by a Varian-Cary 500 spectrophotometer. The unknown concentration was obtained referring to a standard curve using aqueous solutions of caffeic acid at known concentration (900 μM, 600 μM, 500 μM, 300 μM, 150 μM, 70 μM). The quantification of NAC loading efficiency were performed using an Agilent HP 1200 liquid chromatograph (Agilent Technologies, Germany), consisting of a binary pump, an autosampler and a thermostated column compartment. Chromatographic separations were carried out using a Discovery HS-F5 column (150 mm × 2.1 mm, 3 μm) purchased from Sigma–Aldrich (Milan, Italy). The HPLC analyses were carried out using an elution profile composed of an isocratic step water (formic acid 0.1 %):ACN 95:5 at 25 °C. The column was washed with 90 % of acetonitrile for 2.5 min followed by the equilibration of the column for 5 min with 5 % ACN. The flow rate was 0.3 mL/min. The injection volume was 20 μL. An Agilent 6410 triple quadrupole-mass spectrometer with an electrospray ion source operated in positive mode was used for detection. Flow injection analysis was used to optimize the fragmentor and source parameters. The optimized source parameters for MS analysis were: drying gas temperature 350 °C and gas flow 10 L/min, nebulizer gas flow pressure 35 psi and capillary voltage 4500 V. The chromatograms were acquired in selected ion monitoring (SIM) of [M + H +] at m/z of 163.2. Five points calibration curve were constructed for NAC in the concentration ranges 3.0–20.0 ng/mL. NAC samples were analyzed diluting $1*10^6$ times.

Ultrastructural analysis of bacteria cells by transmission electron microscopy

Aliquots of the bacterial suspensions were incubated with nanocrystals for 12 and 24 h at 28 °C. Specifically, the following concentration of nano$CaCO_3$ were tested: 1 mg/mL, 100 μg/mL, 10 μg/mL and 1 μg/mL. The non-treated control included the bacterial suspension added with autoclaved sterile water. Following the incubation with nano$CaCO_3$, an aliquot (ca. 50 μL) of each preparation was observed under the electron microscope (FEI MORGAGNI 282D), either by preparing a dip or ultrathin sections. For the dip method, the carbon coated copper/rhodium grids were incubated with treated and non-treated bacterial suspension for 2 min and then rinsed with 200 μL of distilled water. Negative staining was obtained by floating the grids on 200 μL of 1 % w/v uranyl acetate solution. For the preparation of the ultrathin sections, the bacterial suspensions were added with 1.5 % of GELLY-PHORLM (Euroclone), sliced in small pieces and processed as described by Martelli and Russo [43], prior to be observed at the electron microscope using an accelerating voltage of 80 kV.

Administration of fluorescent nanoCaCO$_3$ to plants

Leaf petioles, hardwood mature cuttings and self-rooted olive plantlets grown in perlite substrate, have been used to verify nanoCaCO$_3$ absorption and translocation into the plants through xylem tissues. Briefly, excised petioles were immersed for 12 h in 10 mL of fluorescent nanocrystals, whereas the basal parts of 1 year-old twigs (15 cm long) were soaked for 72 h in a container containing 10 mL of fluorescent nanoCaCO$_3$ suspension, using perlite as inert support. Self-rooted cuttings (20 cm long) were grown for 15 days in perlite watered with 10 mL of fluorescent nanoCaCO$_3$ suspension. Controls consisted of the same plant materials soaked or immersed in water. Longitudinal and transversal sections were manually prepared and then observed, without staining, with a Nikon Eclipse 600 Microscope under fluorescent light, using a filter block for blue-violet fluorescence with a medium excitation filter bandpass and longpass emission filter. Fluorescent nanoCaCO$_3$ were clearly visible into the yellow spectrum with this filters combination.

Results and discussion

Effects of CaCO$_3$ nanocrystals on Xylella fastidiosa cells

Limited experience exists on the potential use of nanotechnological approach against *X. fastidiosa*. Nanofilms of hyaluronan/chitosan assembled by layer-by-layer deposition are proposed as antibacterial surfaces to control the adhesion and growth of Gram negative pathogens, in particular *X. fastidiosa* cells [45]. In this work we studied the interaction between *X. fastidiosa* cells (De Donno strain) and CaCO$_3$ nanocrystals to understand the potential exploitation of these nanocarriers to deliver antimicrobial compounds to control the bacterium in the infected plants. The interaction between *X. fastidiosa* cells and nanoCaCO$_3$ was investigated through ultrastructural analysis by transmission electron microscopy to visualize cells morphology following treatments with nanoCaCO$_3$ at different concentrations and for different incubation periods. The best conditions for evaluating the ultrastructural interactions corresponded to 1 mg/mL of CaCO$_3$ nanocrystals incubated for 24 h with *X. fastidiosa* cells. The cell morphology of non-treated bacterial cells is reported in Fig. 1a. The bacterial cells shown the characteristic Gram negative wall structure consisting of an outer membrane (OM), an inner membrane (IM) and a dense periplasm between the two membranes (D) which contains a thin layer of peptidoglycans [46]. It is also evident the wrinkled structure typical of this bacterium. Progressive changes of bacteria wall are linked to cells senescence as reported by Mollenhauer and Hopkins during the degenerative progression the intermediate layers become uniformly dense and the dense material zone (D) become difficult to be distinguish by the two membranes (OM and IM) [47]. Figure 1b–f shows the TEM images of the thin sections of *X. fastidiosa* exposed to 1 mg/mL of nanoCaCO$_3$ for 24 h. The main visible effect was the alteration of the bacterial wall complex with an evident detachment of the two membranes that in some cases resulted in the complete destruction of the cell structure. The morphological changes with moderate destructions on cell membranes have been previously described for a Gram negative plants pathogen treated with Ag nanoparticles (AgNPs) [48]. Indeed, various studies have demonstrated that the AgNPs toxicity against bacteria involved both the direct action of nanoparticles and the effects of silver ions release. The interaction of nanoparticles with bacterial cells caused change in membranes morphology and permeability. Furthermore the presence of surfactants on nanoparticles surface was proven to be crucial for biomolecules attach and toxicity mechanism [49]. In our study, deleterious effects on bacterial membranes were recorded upon the use of the nanoCaCO$_3$ without any surface modifications. Furthermore, it is known that ions such as Ca^{2+} and Mg^{2+} are involved in cell-to-cell adhesion, thus the use of nanomaterial based on CaCO$_3$ could have direct effects on bacterial cells viability, even without loading any specific antimicrobial compounds. Indeed, micro and nanoCaCO$_3$ had a strong affinity for various sugar-based polymers such as dextran, chitosan

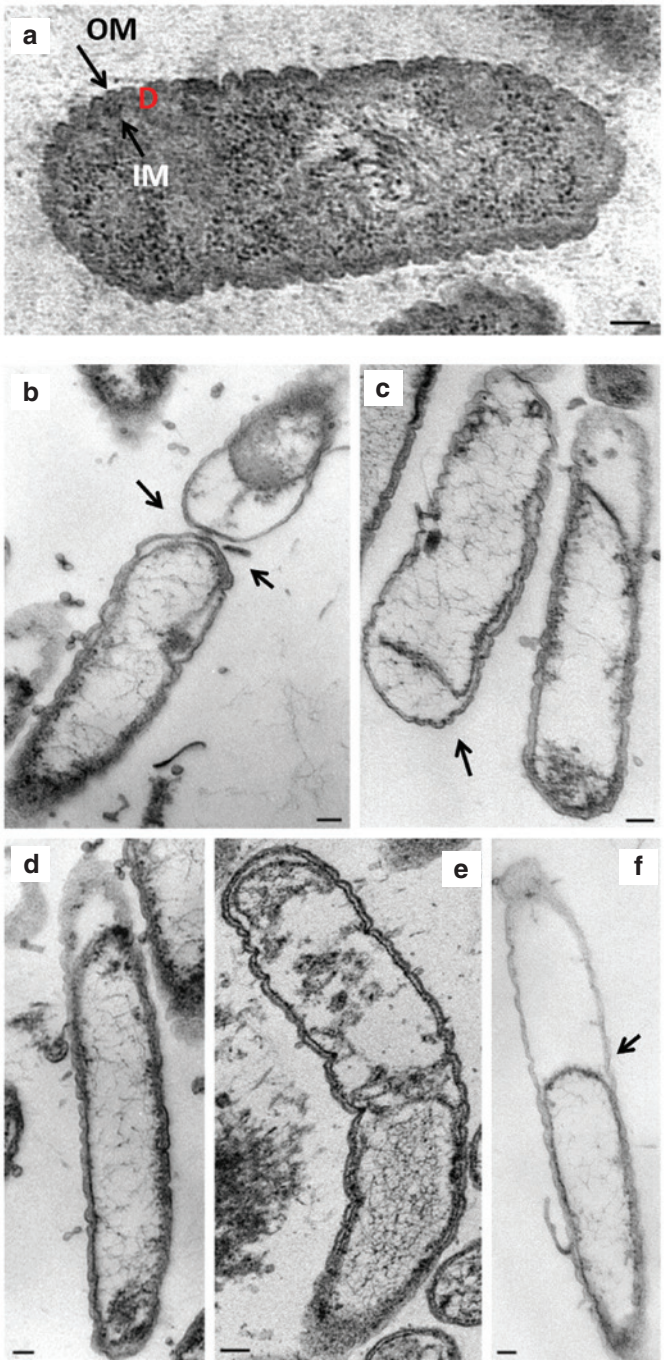

Fig. 1: Thin sections observed at the electron microscope. (a) TEM images of *X. fastidiosa* control cells; (b–f) cells exposed to 1 mg/mL of nanoCaCO$_3$ for 24 h. In Fig. 1a the characteristic cell morphology of *X. fastidiosa* is shown. The black arrows indicate the membranes detachment following nanoCaCO$_3$ interaction. Scale bars: 100 nm.

and pectin, due to the negative z-potential [32, 33]. Therefore nanoCaCO$_3$ could potentially bind bacterial exopolysaccharides.

Furthermore, bacterial cells produced spheroid particles ranging in size from 20 to 50 nm, in presence of nanoCaCO$_3$, as shown in Fig. 2. It is well known that Gram negative bacteria produce Outer membrane vesicles (OMVs) which are spheroid particles, 20–250 nm in size, with different modulating functions: immune response, trafficking and release of extracellular molecules which play important roles in interactions with

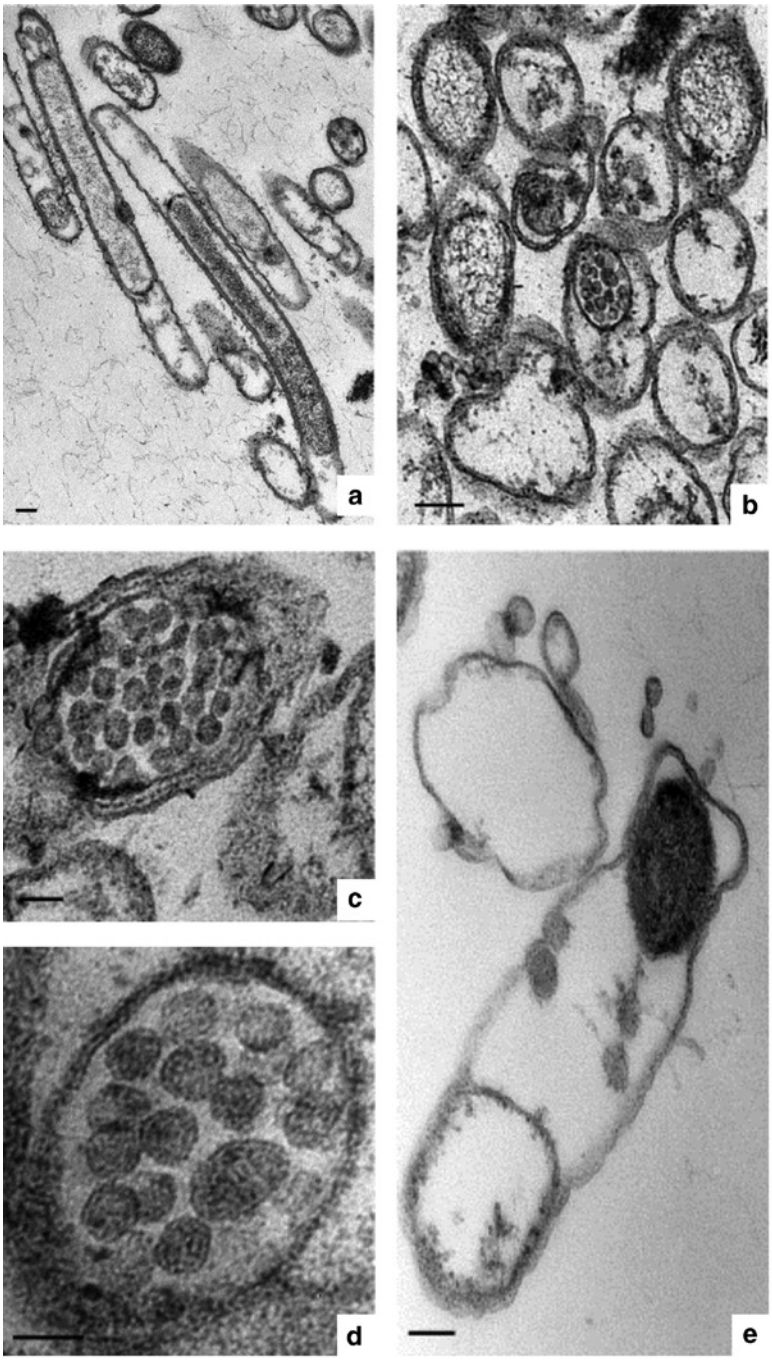

Fig. 2: Electron micrographs of *X. fastidiosa* thin sections. Bacteria cells were exposed to 1 mg/mL of nanoCaCO$_3$ for 24 h. A production of spheroid particles ranging from 20 to 50 nm in size, is clearly evident. Scale bars: (a,b) 250 nm, (c–e) 100 nm.

the habitat such as stress responses [50]. A recent study have demonstrated that *X. fastidiosa* is an active producer of OMV-like nanoparticles functioning as anti-adhesive agents inhibiting biofilm formation and colonization in vitro and in planta [51]. The hypothesis that the disruption of the membranes determine the production of OMV-like nanoparticles has been previously demonstrated in other studies. This was also observed under our experimental conditions: abundant OMV-like nanoparticles inside and outside the cells were observed (Fig. 2). These vesicles were numerous around degenerative cells (Fig. 2e). This interesting evidence about the interaction *X. fastidiosa*-NanoCaCO$_3$, supported the idea of the potential use of nanocrystals

as carriers for control of bacterial infections. To this end, fluorescent-labeled nanoCaCO$_3$ were produced and tested to verify the translocation in planta and two anti-*X. fastidiosa* compounds were loaded to test nanocrystals effectiveness as carriers for antimicrobial compounds.

Phytodrugs loading efficacy

The properties and applications of CaCO$_3$ depend on its morphology, particles size, crystals phase and growth. We have reported a semi-industrial process to obtain calcite nanocrystals without use of organic additives [33]. The porous structure of CaCO$_3$ nanocrystals resulted achieve the drug loading and the efficient polymers or molecules adsorption [31–34]. TEM imaging had allowed to observe the characteristic porous structure of CaCO$_3$ surface as well illustrated in our previous work. We have also revealed a surface area of 4.22 m^2/g (through BET analysis) that favored the physical adsorption [32]. The porous structure of carriers acted as a sponge facilitating molecules adsorption. These crucial features are exploited for two selected phytodrugs entrapping. The loading of caffeic acid was performed at neutral pH and at four different concentrations in line with the in vitro tests which are reported in literature [41]. Maddox et al. verified that the di- and tri-hydroxyl phenolic acids, caffeic acid and gallic acid, were more active than the mono-hydroxyl phenolic acid. Particularly, catechol, caffeic acid and resveratrol had a very strong inhibitory activities. Although, caffeic acid and catechol are the cheapest and therefore the most applicable in agriculture. The Supplementary Figure 1a reports the standard curve that is used for the quantification of caffeic acid concentration in the supernatants. The loading efficacy is more than 50 % with an increasing trend respect to the initial concentration; an efficiency of 82 % is achieved at the maximum tested concentration of 800 μM (Supplementary Figure 1b). This trend of caffeic acid is mainly due to its poor solubility in cold water, so the physical absorption on nanocrystals surface is favored respect to the permanence in the external aqueous environment. NanoCaCO$_3$ have already shown a good ability to trap lipophilic compounds such as phospholipid functionalizations and cancer drugs [32–34]. The positive charge of these nanocrystals provided an efficiency of two phospholipids adsorption near to 100 % [32]. Hydrophobic interactions occurred between nano-crystals and caffeic acid. The initial concentration of 800 μM was used for the preparation of the tested samples. In the case of NAC, two concentrations were tested, in line with the reference study [42]. Muranaka et al. investigated the efficacy of NAC against *X. fastidiosa* for CVC disease with in vitro test and in planta experiment using organic fertilizers as adsorbing substrate. For in vitro study the tested concentrations were 1–2–6 mg/mL. The selected ratio between NAC and fertilizers was 2 g/kg, using 300 mg of NAC-loaded fertilizer for each plants treatment. So, the loading of NAC on nanoCaCO$_3$ was investigated at 6–20 mg/mL. The loading surnatants were analyzed by HPLC-MS and the % loading efficacy was calculated as described in the experimental section. The surnatants concentration was derived from a calibration curve that is reported in Supplementary Figure 1c. An example of chromatogram is shown in Supplementary Figure 1d. The resultant mg of NAC encapsulated were used to calculate the loading capacity considering that the tested quantity of nanoCaCO$_3$ is 100 mg in a volume of 5 mL. This parameter is important for the comparison with the in planta experiment mentioned above. The initial solution of NAC 6 mg/mL shown a loading efficacy of 98.6 % and a loading capacity of 30 %. The initial concentration of 20 mg/mL (a ratio of 1:1 between mg nanoCaCO$_3$ and mg NAC) given a loading efficacy and capacity of 79.5 %. These results indicate that the optimal loading conditions for in planta experiments are 100 mg of nanoparticles, 100 mg of NAC (5 mL of a NAC solution of 20 mg/mL). NAC is a small molecule and its solution is able to saturate the core interstices of nanoCaCO$_3$. The NAC loading was realized by the capillary force due to the nanoporous structure of the particles. Its polar nature advanced the interaction with nanoCaCO$_3$. The controlled drug release from nanoCaCO$_3$ carriers can be triggered in response to different extracellular or intracellular stimulus. NanoCaCO$_3$ is a material susceptible to pH so the acid conditions of cancer microenvironment and cellular lysosomes provided the drug release for human cells applications such as antitumoral therapy [34]. The xylem flow normally has a pH of 5.5 that could promote the controlling release of phyto-drugs following the gradual dissolution of nanoCaCO$_3$. However, pH changes in root and xylem sap can occur in response to several different types of stress such as infection. So NAC and caffeic acid

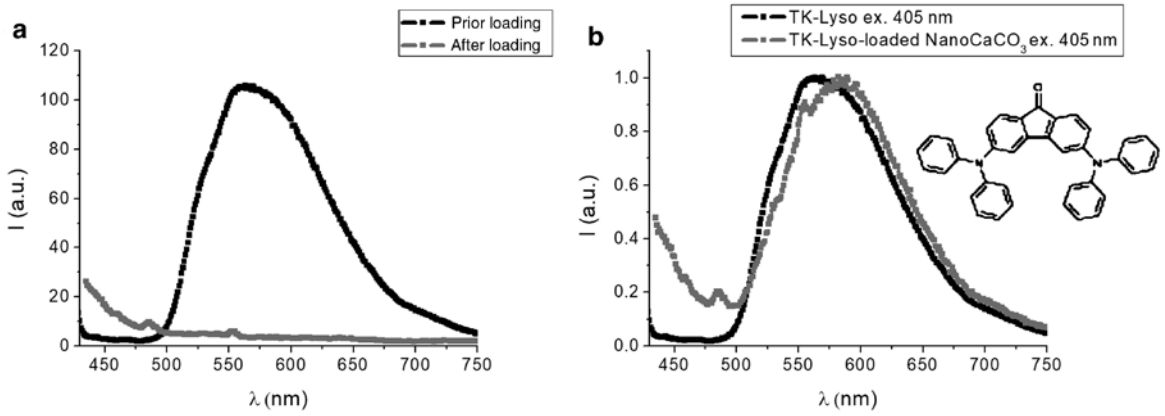

Fig. 3: Fluorescence spectra of dye solution prior and after loading on nanoCaCO$_3$, highlighting the high loading efficacy (a); fluorescence spectra at the excitation wavelength of 405 nm of dye solution and dye-loaded crystals solution (b). In Fig. 3b the chemical structure of TK-Lyso dye is reported.

release in the infected xylematic vessels is a multifactorial topic. Finally, a solution of CaCO$_3$ in constant pH gradient conditions has a predicted pKa of 9 that provides a slow but constant tendency to dissolution allowing loaded molecules release.

NanoCaCO$_3$ in planta application

The CaCO$_3$ nanocrystals investigated in this work have been widely validated as excellent carriers for drug release. Briefly, nanoCaCO$_3$ occur in the crystal phase calcite resulting in a very stable nanosuspension of carriers. Dried CaCO$_3$ nanocrystals were influenced by relative humidity of powder. The dried powder obtained after synthesis suffered phenomenon of crystals growth forming elongated crystals as verified by transmission microscopy. This problem was solved through water removal with isopropanol. Nanoparticles physical-chemical proprieties remained unchanged for a long time of storage at room temperature [52]. They are able to successfully across biological membranes as verified by confocal and electron microscopies addressed to human cells study. Different nanomaterials have demonstrated the ability to go through biological barriers, but some of these could produce cellular toxic effects due to induced osmotic imbalances [26–28]. Our previous reports have demonstrated that nanoCaCO$_3$ are efficiently internalized by human cells without any effect on the cell viability or on the cells structure [32–34]. These results supported the safety of the selected system and the nanoCaCO$_3$ exploitation for phytodrugs delivery in sick plants. The use of nanocarriers is crucial for the improvement of phytodrugs formulations bioavailability. Generally, the application of pesticides require the use of organic solvents, such as toluene or xylene, thus the new formulations are projected for using nano-suspensions in aqueous solutions in stable and safe conditions [4, 5]. Tested nanoCaCO$_3$ could provide all these advantages with low environment impact. The first set of experiments that was carried out in our study aimed to evaluate the uptake and the potential translocation of these carriers into olive plants.

Evidence of uptake and translocation in target plants

Xylella fastidiosa is a xylem-limited pathogenic bacterium capable of inducing in some cases, like in olives, severe diseases with irreversible phenomena of desiccation, mainly resulting from the occlusions of the xylem vessels by the aggregates of bacterial cells and biofilm. Thus, it is fundamental that applications for therapeutic purpose reach the vessels to be effective against *X. fastidiosa*. To this end, CaCO$_3$ nanocrystals represent a good tool, being of small size (75 nm), having good stability in aqueous solutions and capacity

to cross cell membranes [33]. The functionalization of $CaCO_3$ nanocrystals with a fluorescence dye, allowed to assess the capability of the roots to absorb and translocate into the xylem tissues this nanomaterial. A fluorescent probe able to provide biocompatibility and clear photostability was used to ensure detectability of the signal during the whole duration of the experiment (up to 15 days) [44]. The TK-Lyso dye was efficiently adsorbed on nano$CaCO_3$ surface due to its high hydrophobicity establishing hydrophobic interactions (Fig. 3a). This physical absorption is very stable over time and the fluorescence signal of dye-loaded nano$CaCO_3$ is superimposed with that of the dye alone (Fig. 3b). In Fig. 3b was reported the chemical structure of TK-Lyso dye that was prepared by a C–N cross-coupling reaction in a microwave reactor; the optical proprieties were well studied in different conditions as described in previous work [44].

The use of fluorescent nanocrystals clearly demonstrated they were efficiently uptaken and translocated into the vessels of the olive plantlets and cuttings used in our study. In fact, fluorescent nanocrystals were detected in the petioles of the leaves collected from the cuttings immersed into the aqueous suspension of fluorescent nano$CaCO_3$, demonstrating the i.e. uptake by capillarity. Supplementary Figure 2 shows cross sections of the lamina collected from cutting immersed in water (untreated control) or into a fluorescent nanoparticles solution. In the samples treated with fluorescent nanocrystals, the observation of fluorescent spots indicates the presence of nano$CaCO_3$. In Fig. 4 are shown the longitudinal (a–c) and cross (d–g) sections of olive twigs, exposed or not to nano-suspension for 72 h. The specific orange-colored patterns, that was visualized only in the longitudinal sections of treated cuttings, indicated the presence of nano$CaCO_3$ inside the plant vessels (Fig. 4b,c). The cross sections images further confirmed the presence of fluorescent nanoparticles inside the vessels. The treated samples shown the specific orange-colored vacuolar rings, which were absent in the sections of untreated cuttings (Fig. 4e,f). The magnification in Fig. 4g shows the fluorescence signal in the vascular bundles.

These results indicated that nano$CaCO_3$ are able to translocate into xylem vessels and thus $CaCO_3$ nanocrystals are suitable nanocarriers for the delivery of specific antimicrobial compounds against *X. fastidiosa*. It is important to understand whether nanocarriers are able to spread inside the plants, in order to reach each potential accumulation site of pathogen. In literature, many works are reported about the uptake, translocation and localization in plants for different nanoparticles such as metal nano-oxides, CuO, ZnO, TiO_2, but the actual assumption is not always verified. Nanoparticles of Fe_3O_4 are able to be directly uptaken

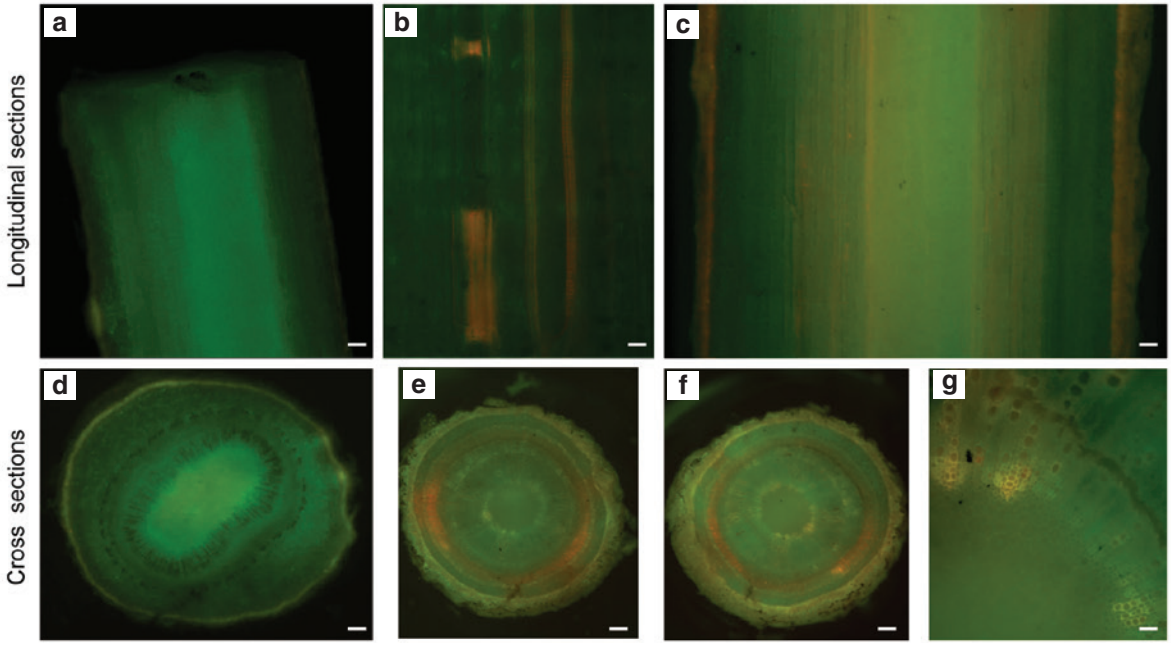

Fig. 4: Longitudinal and cross sections of olive twigs untreated (a, d) and treated (b, c, e, f, g) with fluorescent nano$CaCO_3$. Scale bars: (a, d, e, f) 200 μm; (b, g) 50 μm; (c) 20 μm.

by pumpkin (*Cucurbita maxima*) with no toxicity and they are translocated in specific tissues under magnetic field at a concentration of 0.5 g/L. Other types of nanomaterials such as fullerene, carbon nanotubes and silica nanoparticles are able to across plants barriers, root tissues, cuticles, etc. [28]. The uptake and translocation of nanoparticles by biological systems require the crossing of many chemical and physiological barriers which occurs as a sort of selection by size. In the plant system the transport of water and solutes across a tissue or organs is mediated by apoplastic and symplastic transport pathways. The first allows the passage of particles in the range 5–20 nm, although the second mechanism depends to plasmodesmata diameter in the range of 3–50 nm. Particles with diameter up to this last range can also across this barrier. However, nanoparticles can be internalized by plants cells trough endocytosis. Some authors reported the uptake of larger particles which is due to stress effects influenced by environment, virus but also by particles themselves. Metal nano-oxides are able to produce pores in cell barriers, ruptures on cuticles, allowing their passage and transport [27]. These size exclusion limits not affected the nano$CaCO_3$ uptake as their dimensions are within the range of 50–75 nm in line with the potential symplastic transport pathways and/or endocytosis mechanism. Olive rooted cuttings are studied in order to evaluate the roots mediated uptake of our carriers. These olive seedlings were exposed to 1 mg/mL dye-loaded nano$CaCO_3$ aqueous suspension in sterilized perlite and then worked for microscopy analysis after 15 days. Different plants sections were collected and observed to search the presence of nanocrystals: longitudinal section of the roots, cross-section of the stem, cross and longitudinal section of leaf rib, longitudinal section of leaf inferior lamina. The observation of the leaf sections showed the fluorescence signal from nano$CaCO_3$ both in the xylem portion (vessels of primary rib and petiole) and in parenchymatic tissues (cuticle and epidermis). These observations were carried out by the microscopic images reported in Fig. 5. In Fig. 5a,b are highlighted the cuticle with the upper and lower epidermis layers. The localization of nanocrystals was evident both in the epidermis and in the cuticles suggesting a homogeneous distribution in the plant tissues. The Fig. 5c–f report the cross and longitudinal section of leaf rib; we observed nano$CaCO_3$ in the treated sample, indicating the transport through the vessels up to the foliar tissue.

Observations were then extended to roots and stems sections. The images of roots longitudinal section after 15 days of treatment are shown in Fig. 6a,b. In this case the difference between treated and untreated samples is less evident because most of the nanocrystals had already translocated into the stem and leaves. Observations of the radial sections of the stems deriving from uptake sample clearly showed the presence of orange-colored spots corresponding to the fluorescent crystals (Fig. 6d). These were absent in the non-treated samples (Fig. 6c). A close up of a longitudinal section of the stem with the fluorescent nano$CaCO_3$ is reported in Supplementary Figure 3.

The overall results of these microscopy observations indicated that $CaCO_3$ nanocarriers can be adsorbed by olive roots and can be transported through the xylem vessels reaching different plant tissues, thus they could potentially act against pathogens infecting different tissues of the plants.

Testing nano$CaCO_3$ under greenhouse conditions

After demonstrating the capability of olive plants to adsorb and translocate fluorescent nanocrystals, in planta experiments were set to test their use as carriers of different antimicrobial compounds. Various studies have investigated the role of different molecules in the pathogen homeostasis to design efficient treatments for infected crops. In particular, the role of mineral elements was revealed crucial in *X. fastidiosa* cells. Some minerals, such as Cu and Zn, act as stress factors reducing planktonic cells growth and biofilm formation [39]. Zn and Cu complexed with citric-acid hydracids have revealed a statistically significant reduction of *X. fastidiosa* cells both in vitro and in planta tests [51]. Nano$CaCO_3$ were loaded with two compounds which in previous works were proven to have activity against different strains of *X. fastidiosa* [41, 42]. NAC is a great anti-biofilm agent as verified by experiment for Citrus Variegated Chlorosis disease, also caused by *X. fastidiosa*. Phenolic compounds effectively inhibit pathogen growth. The caffeic acid shown a minimum inhibitory concentration (MIC) of 200 μM against four *X. fastidiosa* strains. Only one work about a nanotechnological

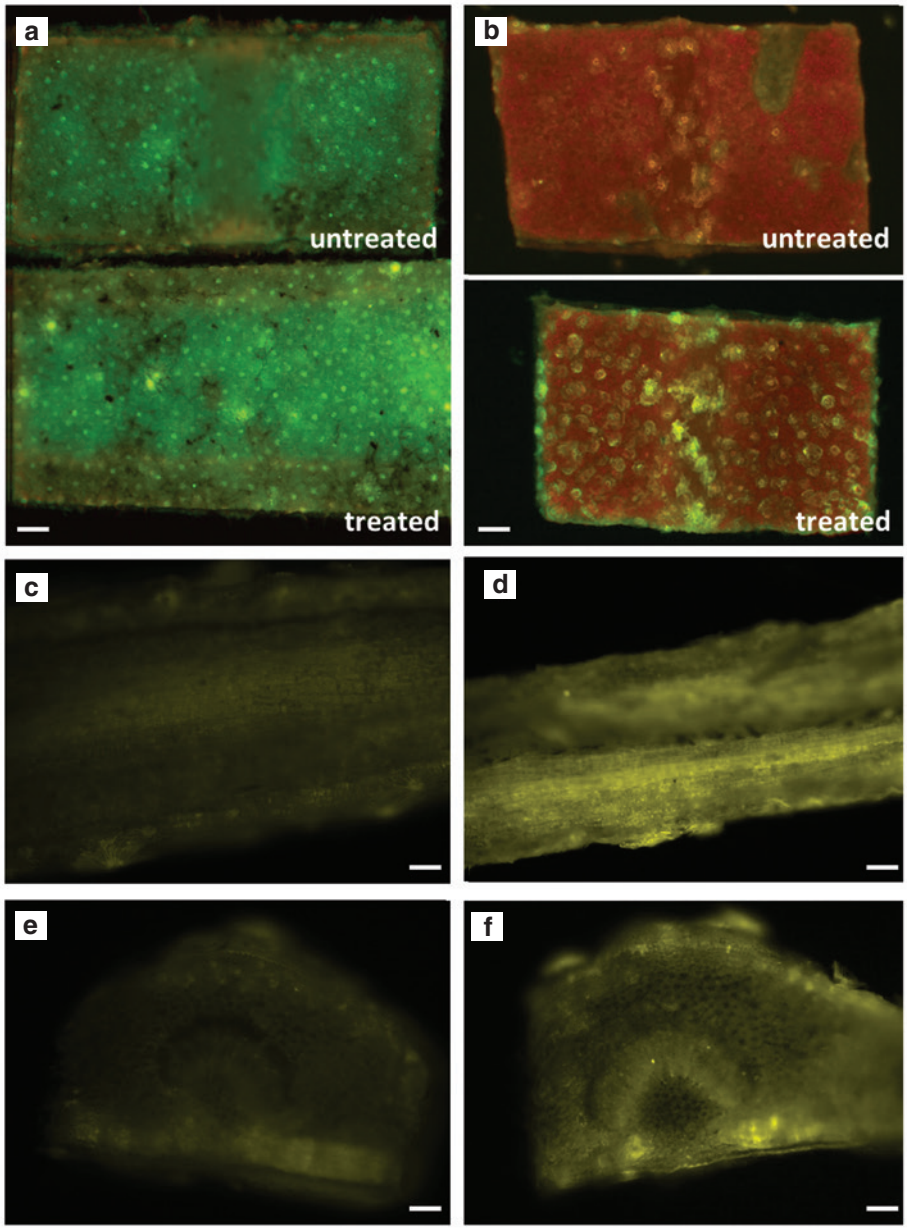

Fig. 5: Fluorescence microscopy images of the upper (a) and lower (b) surface of olive leaf, longitudinal (c) and cross (e) section of midrib from untreated sample; longitudinal (d) and cross (f) section of midrib from a treated sample. Scale bars: (a, b) 200 μm; (d, e, f) 50 μm; (c) 20 μm.

approach against *X. fastidiosa* is reported in the literature. Nanofilms of hyaluronan/chitosan assembled by layer-by-layer are proposed as antibacterial surfaces to control the adhesion and growth of *X. fastidiosa* [45]. We have developed a safe and pre-industrial process for producing nanocrystals of $CaCO_3$ without organic solvents or other additives [33]. The porous structure of $CaCO_3$ particles makes these nanocrystals suitable for drug loading and polymers or molecules adsorption [32–34]. In our experiments, the efficacy of loading on nano$CaCO_3$ was high for both compounds, NAC and caffeic acid. Nano$CaCO_3$ have been proven to be smart delivery systems for anticancer drugs. In our previous work we found an anti-proliferative effect of drug-loaded nano$CaCO_3$ higher than free drug at the same nominal concentration [34]. In this work, we made attempts to set a protocol for the administration of phytodrugs-loaded nanocarriers to olive plants infected by *X. fastidiosa*. However, due to difficulties and the long time required to prepare infected experimental olive

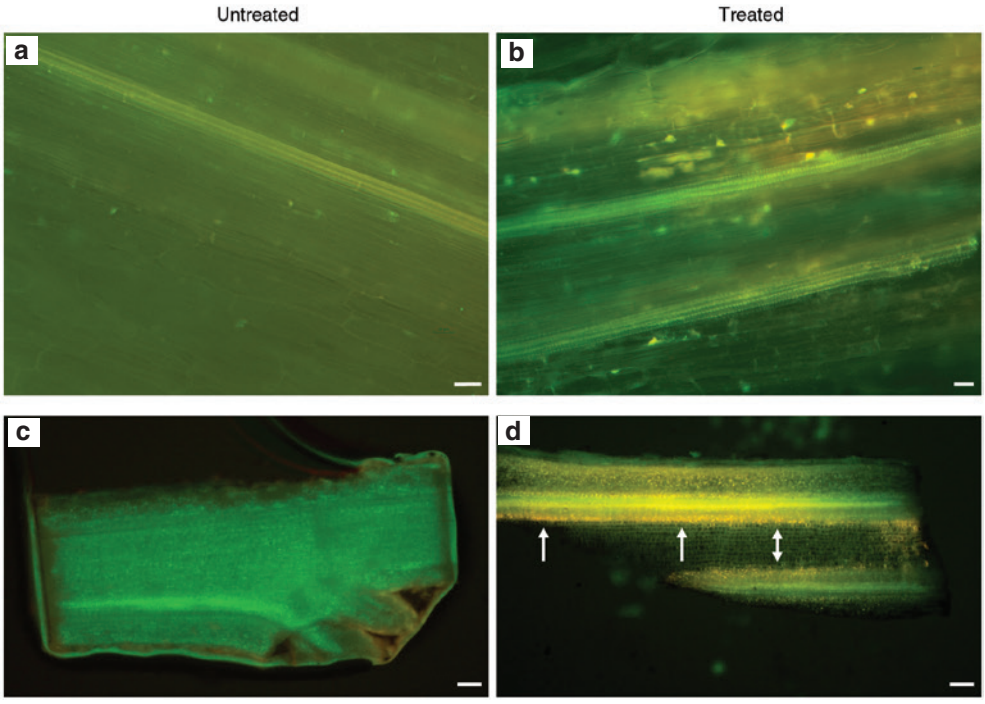

Fig. 6: Fluorescence image of primary roots (a, b) and stems radial sections (c, d); the white arrows indicated the nano$CaCO_3$ in stem of treated sample. Scale bars: (a, b) 20 μm; (c, d) 200 μm.

plants, these initial experiments were conducted on a limited number of replications. Tetracycline was used as reference control (knowing the efficacy of this antibiotic compound); whereas the untreated control was irrigated only with water. Plants were irrigated also with pure nano$CaCO_3$ suspension in order to verify the potential effect of non-loaded nanocarriers. The plants treatments were performed as described in the experimental section. The data collected upon testing the presence and the size of the bacterial populations in the treated plants and in the controls showed initial bacterial concentrations in the average range of 10^5 CFU/mL, which slightly increased, regardless the different treatments, over the time as the infections progressed. As shown in the Supplementary Tables 1, 2 months after the treatments the bacterial population size did not vary from the initial concentration and in some plants started to show symptoms of severe desiccations, typically developed by susceptible olive cultivars upon infections with the Apulian strain of *X. fastidiosa*. No significant differences, in terms of population size, were recorded among the different treatments. These data indicate that additional efforts to set experiments by varying different parameters (n. of applications, doses, duration of the application, etc.) are needed. Furthermore, the lack of positive results confirm the notorious difficulties for the control and for the application of effective therapeutic tools for *X. fastidiosa*.

Conclusion

The interactions of nanomaterials with living systems depend on their physicochemical features including size distribution, shape, surface area, crystallinity, agglomeration state, surface charge. $CaCO_3$ particles have generally excellent properties for improvement of many materials in various sectors such as plastics, paper, environmental tools, biosensors and drug delivery. $CaCO_3$ is a natural occurring and abundant mineral and it can exist in mainly four polymorphs: calcite, vaterite, aragonite and amorphous calcium carbonate; calcite is the most thermodynamically stable phase. Many techniques to produce $CaCO_3$ micro and nanoparticles are reported in literature [1]. The challenge is to tune the specific morphology, the crystal structure, particles size

and charge in order to obtain final specific applications. In particular, the biocompatibility and non-toxicity of $CaCO_3$ makes it an attractive drug delivery vehicle. We have demonstrated an effective targeted delivery of drugs for cancer therapy using nano$CaCO_3$. $CaCO_3$ crystals resulted achieve the drug loading and the efficient activity of drug [31, 34]. In this work, we tested the possibility to use these nanocarriers for controlled release of antimicrobial agents against *X. fastidiosa*. Recently, the exploitation of $CaCO_3$ nanocrystals for the controlled release of an antibiotic proved to increase the antibacterial activity [53]. The recent bibliography underlines the use of nanomaterials as innovative tools for sustainable protection of crops [5, 54–56]. Our idea was to capitalize the great physicochemical and biological features of $CaCO_3$ nanocarriers to fight against a vascular plant pathogen, *X. fastidiosa* currently causing a severe epidemic in olive trees in southern Italy [37]. To this end, we first investigated the in vitro interactions between carriers and *X. fastidiosa* finding an alteration of bacteria wall. Here, we assessed the capability of plants to uptake and translocate nanocrystals, and ultimately we tested the possibility to deliver into the xylem of olive plants different compounds using nano-$CaCO_3$. Using fluorescent nano$CaCO_3$, we tested and confirmed the hypothesis that these nanocrystals can be adsorbed by the roots and then can be effectively translocated into the plants vessels and other tissues. This evidence confirms that different compounds (phytodrugs, fertilizers) can be delivered and released into the plants using these nanocarriers. In our studies we showed that nano$CaCO_3$ were able to efficiently encapsulate antimicrobial, bactericidial and antibiofilm substances (i.e. NAC and caffeic acid). We performed experiments for investigating the in planta efficacy of the loaded nano-formulations under greenhouse conditions. Although the results of these applications are limited in terms of replications and reproducibility and thus the preliminary data are not sufficient to draw any solid conclusion about the use of nano$CaCO_3$-based phytodrugs to cure *X. fastidiosa* infections, they allowed to define suitable experimental conditions for more extensive testing to be carried out in the future, i.e. testing other potential anti-*X. fastidiosa* agents.

Acknowledgments: We thank Prof. Giorgio Mariano Balestra for critical reading and helpful reviewing of the manuscript. We also thank Dr. Maria Saponari for providing the bacterial strain of *Xylella fastidiosa* and review the discussion of results. Project "Tecnologie Abilitanti per Produzioni Agroalimentari Sicure e Sostenibili-T.A.P.A.S.S". Cluster Tecnologici Regionali 2014-PELM994 (CUP B38C14002040008). Project "Trattamenti Fitoterapici innovAtivi a base di veTtori di chitosAno-FATA", Bando pubblico di ricerca per la presentazione di proposte progettuali Cod. A, n. 1410 del 12 giugno 2015 "Approvazione delle linee guida per il parco della ricerca e sperimentazione finalizzata alla prevenzione e al contenimento del complesso del disseccamento rapido dell'olivo (CODIRO)" CUP B36J16002170007. Project "Olivicoltura e difesa da *Xylella fastidiosa* e da insetti vettori in Italia – Oli.Di.X.I.It", prot. Mipaaf n.0011485 del 05/04/2017 (Ministero delle politiche agricole alimentari e forestali).

References

[1] Y. Boyjoo, V. K. Pareek, J. Liu. *J. Mater. Chem. A* **2**, 14270 (2014).
[2] N. G. M. Palmqvist, J. M. Nedelec, G. A Seisenbaev, V. G. Kessler. *Acta Biomater*. **57**, 426 (2017).
[3] F. Baldassarre, V. Vergaro, F. Scarlino, F. De Santis, G. Lucarelli, A. della Torre, G. Ciccarella, R. Rinaldi, G. Giannelli, S. Leporatti. *Macromol. Biosci.* **12**, 656 (2012).
[4] J. B. Peters, H. Bouwmeester, S. Gottardo, V. Amenta, M. Arena, P. Brandhoff, H. J. P. Marvin, A. Mech, F. B. Moniz, L. Q. Pesudo, H. Rauscher, R. Schoonjans, A. K. Undas, M. V. Vettori, S. Weigel, K. Aschberger. *Trends Food Sci. Technol.* **54**, 155 (2016).
[5] E. Fortunati, A. Mazzaglia, G. M. Balestra, *J. Sci. Food Agric.* **99**, 986 (2019).
[6] Md. Nuruzzaman, M. M. Rahman, Y. Liu, R. Naidu. *J. Agric. Food Chem*. **64**, 1447 (2016).
[7] D. Tilman, K. G. Cassman, P. A. Matson, R. Naylor, S. Polasky. *Nature* **7**, 418 (2002).
[8] M. M. Rui, C. X. Ma, Y. Hao, J. Guo, Y. K. Rui, X. L. Tang, Q. Zhao, X. Fan, Z. T. Zhang, T. Q. Hou, S. Y. Zhu. *Front. Plant Sci.* **7**, 815 (2016).
[9] H. Chen, R. Yada. *Trends Food Sci. Technol.* **22**, 585 (2011).
[10] J. A. Tapia-Hernández, P. I. Torres-Chávez, B. Ramírez-Wong, A. Rascón-Chu, M. Plascencia-Jatomea, C. G. Barreras-Urbina, N. A. Rangel-Vázquez, F. Rodríguez-Félix. *J. Agric. Food Chem*. **63**, 4699 (2015).

[11] S. Kumar, N. Chauhan, M. Gopal, R. Kumar, N. Dilbaghi. *Int. J. Biol. Macromol.* **81**, 631 (2015).
[12] A. Perez-de-Luque, D. Rubiales. *Pest Manag. Sci.* **65**, 540 (2009).
[13] L. R. Khot, S. Sankaran, J. M. Maja, R. Ehsani, E. W. Schuster. *Crop Prot.* **35**, 64 (2012).
[14] E. E. Hafez, H. S. Hassan, M. F. Elkady, E. Salama. *Int. J. Sci. Technol. Res.* **3**, 318 (2014).
[15] Y. Hao, X. Cao, C. Ma, Z. Zhang, N. Zhao, A. Ali, T. Hou, Z. Xiang, J. Zhuang, S. Wu, B. Xing, Z. Zhang, Y. R. Front. *Plant Sci.* **8**, 1332 (2017).
[16] Z. Zabrieski, E. Morrell, J. Hortin, C. Dimkpa, J. McLean, D. Britt, A. Anderson. *Ecotoxicology* **24**, 1305 (2015).
[17] A. Panáček, M. Kolář, R. Večeřov, R. Prucek, J. Soukupov, V. Kryštof, P. Hamal, R. Zbořil, L. Kvítek. *Biomaterials* **30**, 6333 (2009).
[18] S. W. Kim, J. H. Jung, K. Lamsal, Y. S. Kim, J. S. Min, Y. S. Lee. *Mycobiology* **40**, 53 (2012).
[19] C. Marambio-Jones, E. M. V. Hoek. *J. Nanoparticle Res.* **12**, 1531 (2010).
[20] G. A. Martinez-Castanon, N. Nino-Martınez, F. Martınez-Gutierrez, J. R. Martınez-Mendoza, F. Ruiz. *J. Nanoparticle Res.* **10**, 1343 (2008).
[21] H.-J. Park, S. H. Kim, H. J. Kim, S.-H. Choi. *Plant Pathol. J.* **22**, 295 (2006).
[22] J. S. Min, K. S. Kim, S. W. Kim, J. H. Jung, K. Lamsal, S. B. Kim, M. Y. Jung, Y. S. Lee. *Plant Pathol. J.* **25** 376 (2009).
[23] J. Thiel, L. Pakstis, S. Buzby, M. Raffi, C. Ni, D. J. Pochan, S. I. Shah. *Small* **3**, 799 (2007).
[24] E. Battiston, M. C. Salvatici, A. Lavacchi, A. Gatti, S. Di Marco, L. Mugnaia. *Pest Manag. Sci.* **74**, 1903 (2018).
[25] M. Shenashen, A. Derbalah, A. Hamza, A. Mohamedd, S. El Safty. *Pest Manag. Sci.* **73**, 1121 (2016).
[26] Z. Piperigkou, K. Karamanou, A. B. Engin, C. Gialeli, A. O. Docea, D. H. Vynios, M. S. G. Pavão, K. S. Golokhvast, M. Shtilman, A. Argiris, E. Shishatskaya, A. M. Tsatsakis. *Food Chemi. Toxicol.* **91**, 57 (2016).
[27] K. J. Dietz, S. Herth. *Trends Plant Sci.* **16**, 582 (2011).
[28] P. Wang, E. Lombi, F. J. Zhao, P. M. Kopittke. *Trends Plant Sci.* **21**, 699 (2016).
[29] C. M. Rico, S. Majumdar, M. Duarte-Gardea, J. R. Peralta-Videa, J. L. Gardea-Torresdey. *J. Agric. Food Chem.* **59**, 3485 (2011).
[30] T. Souhoa, L. Lambonia, L. Xiao, G. Yang. *Biotechnol. Adv.* **36**, 1928 (2018).
[31] V. Vergaro, P. Papadia, S. Leporatti, S. A. De Pascali, F. P. Fanizzi, G. Ciccarella. *J. Inorg. Biochem.* **153**, 284 (2015).
[32] F. Baldassarre, C. Allegretti, D. Tessaro, E. Carata, C. Citti, V. Vergaro, C. Nobile, G. Cannazza, P. D'Arrigo, A. Mele, L. Dini, G. Ciccarella. *ChemistrySelect* **1**, 6507 (2016).
[33] V. Vergaro, E. Carata, F. Baldassarre, E. Panzarini, L. Dini, C. Carlucci, S. Leporatti, B. F. Scremin, D. Altamura, C. Giannini, G. Ciccarella. *Adv. Powder Technol.* **28**, 2445 (2017).
[34] V. Vergaro, M. Civallero, C. Citti, M. Cosenza, F. Baldassarre, G. Cannazza, S. Pozzi, S. Sacchi, F. P. Fanizzi, G. Ciccarella. *Cancers* **10**, 31 (2018).
[35] G. Loconsole, O. Potere, D. Boscia, G. Altamura, K. Djelouah, T. Elbeaino, D. Frasheri, D. Lorusso, F. Palmisano, P. Pollastro, M. R. Silletti, N. Trisciuzzi, F. Valentini, V. Savino, M. Saponari. *J. Plant Pathol.* **96**, 7 (2014).
[36] P. J. Zarco-Tejada, C. Camino, P. S. A. Beck, R. Calderon, A. Hornero, R. Hernández-Clemente, T. Kattenborn, M. Montes-Borrego, L. Susca, M. Morelli, V. Gonzalez-Dugo, P. R. J. North, B. B. Landa, D. Boscia, M. Saponari, J. A. Navas-Cortes. *Nat. Plants* **4**, 432 (2018).
[37] M. Saponari, D. Boscia, G. P. Martelli. *Acta Hortic.* **1199**, 251 (2018).
[38] D. L. Hopkins. *Annu. Rev. Phytopathol.* **27**, 271 (1989).
[39] F. Navarrete, L. De La Fuente. *Appl. Environ. Microbiol.* **80**, 1097 (2014).
[40] P. Wang, Y. Lee, M. M. Igo, M, C. Roper. *Mol. Plant Pathol.* **18**, 7 (2016).
[41] C. E. Maddox, L. M. Laur, L. Tian. *Curr. Microbiol.* **60**, 53 (2010).
[42] L. S. Muranaka, T. E. Giorgiano, M. A. Takita, M. R. Forim, L. F. C. Silva, H. D. Coletta-Filho, M. A. Machado, A. A. de Souza. *PLoS One* **8**, 72937 (2013).
[43] G. P. Martelli, M. Russo. *Methods Virol.* **8**, 143 (1984).
[44] A. L. Capodilupo, V. Vergaro, E. Fabiano, M. De Giorgi, F. Baldassarre, A. Cardone, A. Maggiore, V. Maiorano, D. Sanvitto, G. Giglibe, G. Ciccarella. *J. Mater. Chem. B* **3**, 3315 (2015).
[45] J. Hernandez-Montelongo, V. F. Nascimento, D. Murillo, T. B. P. Taketa, Sahoo, A. A. de Souza, M. M. Beppu, M. A. Cotta. *Carbohyd. Polym.* **136**, 1 (2016).
[46] T. J. Silhavy, D. Kahne, S. Walker. *Cold Spring Harb. Perspect. Biol.* **2**, a000414 (2010).
[47] H. H. Mollenhauer, D. L. Hopkins. *J. Bacteriol.* **119**, 612 (1974).
[48] J. N. Chen, S. L. Li, J. X. Luo, R. S. Wang, W. Ding. *J. Nanomat.* **1**, 1 (2016).
[49] C. Schwechheimer, C. J. Sullivan, M. J. Kuehn. *Biochemistry* **52**, 3031 (2013).
[50] M. Ionescu, P. A. Zaini, C. Baccari, S. Tran, A. M. da Silva, S. E. Lindow. *Proc. Natl. Acad. Sci. U S A* **111**, E3910 (2014).
[51] M. Scortichini, J. Chen, M. de caroli, G. Dalessandro, N. Pucci, V. Modesti, A. L'aurora, M. Petriccione, L. Zampella, F. Mastrobuoni, D. Migoni, L. Del Coco, C. R. Girelli, F. Piacente, N. Cristella, P. Marangi, F. Laddomada, M. Di Cesare, G. Cesari, F. P. Fanizzi, S. Loreti. *Phytopathol. Mediterr.* **57**, 48 (2018).
[52] V. Vergaro, E. Carata, E. Panzarini, F. Baldassare, L. Dini, G. Ciccarella. *AIP Conf. Proc.* **1667**, 020014 (2015).
[53] L. F. Cruz, P. A. Cobine, L. De La Fuente. *Appl. Environ. Microbiol.* **78**, 1321 (2012).
[54] X. Pan, S. Chen, D. Li, W. Rao, Y. Zheng, Z. Yang, L. Li, X. Guan, Z. Chen. *Front. Chem.* **5**, 130 (2018).

[55] E. Fortunati, G. M. Balestra. *J. Nanomed. Nanotechnol.* **2**, 115 (2018).
[56] A. Rossetti, A. Mazzaglia, M. Muganu, M. Paolocci, M. Sguizzato, E. Esposito, R. Cortesi, G. M. Balestra. *J. Plant Dis. Protect.* **124**, 563, (2017).

Supplementary Material: The online version of this article offers supplementary material (https://doi.org/10.1515/pac-2018-1223).